RSC Chemical Biology

ROYAL SOCIETY OF CHEMISTRY

PAPER

View Article Online
View Journal

Cite this: DOI: 10.1039/d5cb00289c

Fluorescent cationic fluorinated oxazoliniums for cysteine bioconjugation *via* an S_NAr reaction

Karen Ka-Yan Kung,†[ab] Yosephine Tania Limanto,†[a] Ajcharapan Tantipanjaporn,[a] Jie-Ren Deng,[c] Lai-Yi Tsang[c] and Man-Kin Wong *[ab]

Received 11th November 2025,
Accepted 13th February 2026

DOI: 10.1039/d5cb00289c

rsc.li/rsc-chembio

Using cationic fluorinated oxazolinium compounds, fluorescent cysteine-selective S_NAr bioconjugation proceeds under mild conditions, resulting in fluorescent-labelled peptides and proteins with moderate to excellent conversions of up to 99%. Live cell imaging studies reveal good compatibility of these oxazoliniums as fluorescent dyes for mitochondrial targeting.

Introduction

Fluorescent labelling allows the attachment of fluorophores to biomolecules, resulting in fluorescent bioconjugates with excellent selectivity and functional diversity for visualizing and tracking biological activities.[1–3] Cysteine is commonly used as a handle in bioconjugation due to its high nucleophilicity and relatively low abundance.[1,4] Therefore, different classes of electrophiles, including α,β-unsaturated carbonyls, maleimides and hypervalent iodine compounds, have been developed for cysteine-based modification of peptides and proteins.

Cysteine arylation by fluorinated aromatic compounds *via* nucleophilic aromatic substitution (S_NAr) has demonstrated advantages over metal- or photo-catalyzed arylation.[5,6] Since 2013, Pentelute *et al.*,[7,8] Derda *et al.*,[9] Cobb *et al.*,[10] Wu *et al.*[11] and Harran *et al.*[12] have developed polyfluoroaromatic compounds for cysteine-selective bioconjugation and Cys–Cys stapling of native peptides (Fig. 1a). Recently, pyridinium salts, such as *N*-methyl-*o*-fluoropyridinium iodide (CAP1), showed excellent reactivity due to the cationic nature, water solubility and highly polarized C–F bonds towards rapid thiol arylation (Fig. 1b).[13]

Various advancements have been made in fluorescence analysis using small molecule fluorescent probes including the incorporation of fluorine to fluorophores to improve imaging capabilities, targeting functionalities and overall biological activities.[14–16] To achieve fluorescent cysteine bioconjugation, attachment of a fluorescent dye into the bioconjugation reagents is necessary, requiring additional synthetic effort. Thus, it is interesting to develop a fluorescent bioconjugation reagent without the need for addition of a separate fluorescent dye. Notably, Zhang *et al.* introduced a series of fluorescent polyfluoroporphyrins for the labelling of cysteine-containing peptides and proteins *via* S_NAr reactions, while preserving water solubility, cationic nature and tunable fluorescence (Fig. 1c).[17]

Although many cationic polycyclic heteroaromatics, such as isoquinoliniums, quinoliziniums, and pyridiniums, have been reported as water-soluble fluorophores, very few reports are on the synthesis and applications of oxazoliniums.[18–20] Here, we report a series of fluorescent cationic fluorinated oxazoliniums for cysteine bioconjugation *via* an S_NAr reaction (Fig. 1d). By using rhodium (Rh)-catalyzed reaction, a series of fluorinated

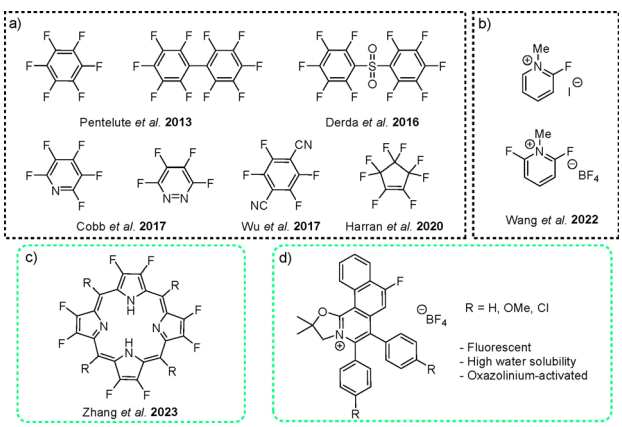

Fig. 1 Fluorinated compounds for cysteine arylation. (a) Polyfluoroaromatic compounds. (b) Pyridinium-activated fluorine. (c) Fluorescent polyfluoroporphyrin. (d) Our fluorescent fluorinated oxazolinium compounds.

[a] Research Institute for Future Food, Department of Food Science and Nutrition, The Hong Kong Polytechnic University, Hung Hom, Hong Kong, China. E-mail: mankin.wong@polyu.edu.hk
[b] Centre for Eye and Vision Research (CEVR), 17W Hong Kong Science Park, Hong Kong, China
[c] Department of Applied Biology and Chemical Technology, The Hong Kong Polytechnic University, Hung Hom, Hong Kong, China
† These authors contributed equally to this work.

oxazolinium compounds were prepared using a modular approach.[21]

Investigation of the photophysical properties and applications of the fluorinated oxazoliniums for cysteine bioconjugation and live cell imaging was performed.

Results and discussion

Design and synthesis of oxazoliniums

Based on our previous study on the development of polycyclic quinoliziniums[22–24] and oxazoliniums,[25] oxazolinium **oxa-1** was first synthesized *via* a Rh-catalyzed C–H annulation between oxazoline **S1a** and diphenylacetylene **S2a** in the presence of silver salt (Scheme 1). Oxazolinium **oxa-1** was characterized by NMR and mass spectrometry (SI).

We initiated the study through the reaction of **oxa-1** (10 equiv.) with cysteine-containing peptide **1** (STSSSCNLSK) (0.1 mM, 1 equiv.) for 18 h at room temperature (Scheme S1, SI). By utilization of LC-MS to determine the conversion, we found that reaction at room temperature led to a moderate conversion of 61% of modified peptide **1a** (Fig. S13, SI). To improve the conversion, the reaction mixture was heated at 40 °C for 18 h. Unexpectedly, 75% of peptide **1** was converted to the hydrolysed product **1a′** (Fig. S15, SI). In addition, dimerization of the native peptide **1** increased from 9% to 23% at room temperature. As the C2 carbon atom of the oxazoline is susceptible to nucleophilic attack,[26] **oxa-2–4** were designed with geminal dimethyl groups to overcome the hydrolysis of the target product.

Optimization of the peptide modification reaction conditions

Treatment of the peptide **1** with **oxa-2** (10 equiv.) at room temperature gave a moderate conversion of 66% and 10% dimerization (Table 1, entry 1). Upon heating of the reaction mixture at 40 °C, a significant increase to 86% conversion was observed (entry 2). As dimerization of the peptide was a competing reaction to the cysteine arylation, TCEP (a reducing agent) was added to inhibit the dimerization (entry 3). Optimization of the reaction conditions was conducted by screening different conditions and varying the amount of **oxa-2** and TCEP (entries 4–9). To our delight, up to 96% conversion was attained when only 5 equivalents of **oxa-2** and 1 equivalent of TCEP were utilized under heating at 40 °C (entry 7).

With the optimized conditions in hand, a time course study was conducted. Up to 95% conversion was obtained within 16 h of reaction before reaching a plateau (Fig. S1, SI). Peptide **1** was

Table 1 Optimization of the cysteine arylation reaction conditions[a]

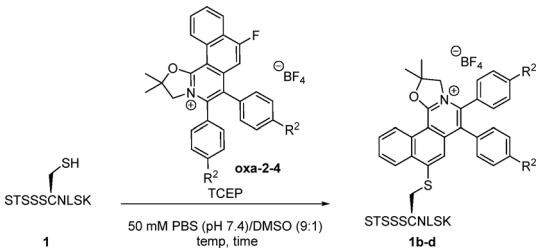

Entry	Compound (equiv.)	TCEP (equiv.)	Temp. (°C)	Time (h)	Product	Conv.[b] (%)
1	**oxa-2** (10)	0	rt	18	**1b**	66
2	**oxa-2** (10)	0	40	18	**1b**	86
3	**oxa-2** (10)	10	rt	18	**1b**	64
4	**oxa-2** (10)	10	40	18	**1b**	94
5	**oxa-2** (5)	5	40	18	**1b**	95
6	**oxa-2** (5)	2	40	18	**1b**	96
7	**oxa-2** (5)	1	40	18	**1b**	96
8	**oxa-2** (3)	1	40	18	**1b**	91
9	**oxa-2** (1)	1	40	18	**1b**	89
10[c]	**oxa-3** (5)	1	40	16	**1c**	90
11[c]	**oxa-4** (5)	1	40	16	**1d**	99
12[c]	**S1b** (control) (5)	1	40	16	**1e**	0

[a] Reaction conditions for modification: Treatment of peptide **1** (0.1 mM) with **oxa-2** in the presence of TCEP, in 50 mM PBS buffer (pH 7.4)/DMSO (9 : 1). [b] Conversion of the modification was determined by LC-MS/MS analysis. [c] Optimized conditions following time-course study, **oxa-3**, **oxa-4** and oxazoline **S1b** were utilized.

then treated with electron-donating substituted **oxa-3** and electron-withdrawing substituted **oxa-4**, leading to 90% and 99% conversion respectively (entries 10 and 11). The higher conversion obtained from the electron-withdrawing **oxa-4** compared to **oxa-2** and **oxa-3** is possibly due to the higher electrophilicity of the cation due to the –Cl substituent. Furthermore, as a proof of concept, no target product was observed when peptide **1** was treated with oxazoline **S1b** as a control (entry 12). This observation indicated that cysteine arylation is enhanced by the cationic nature of the oxazolinium electrophiles and highly polarized C–F bonds.[13]

Model reactions of peptide modifications

Model reactions were conducted by treatment of **oxa-2–4** (0.1 mmol, 1 equiv.) and *N*-Boc cysteine methyl ester (1.5 equiv.) at room temperature for 16 h to give **oxa-5–7** (Scheme 2). By using mass spectrometry, no starting **oxa-2–4** were observed in

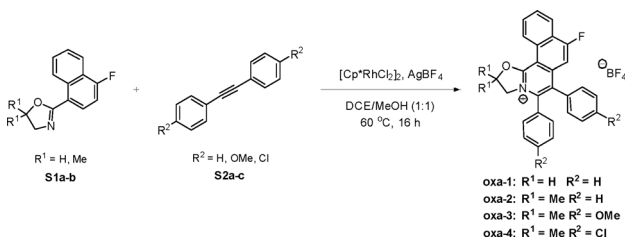

Scheme 1 Synthetic procedure of **oxa-1–4**.

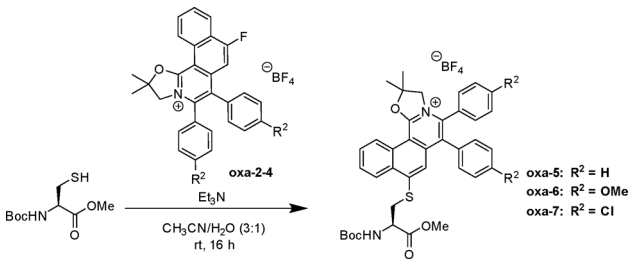

Scheme 2 Model reactions of cysteine arylation using *N*-Boc cysteine methyl ester.

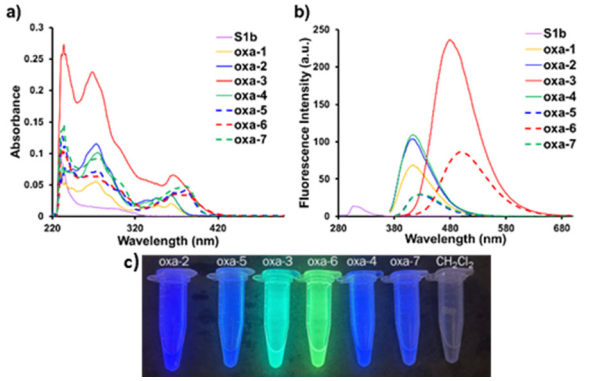

Fig. 2 (a) Absorption spectra and (b) fluorescence spectra of oxazoline **S1b** and **oxa-1–7** (1 μM in CH_2Cl_2). (c) Fluorescence images of **oxa-2–7** and solvent (control) under a 365 nm UV lamp (1 mM in CH_2Cl_2).

the crude mixture, indicating complete consumption of the starting oxazolinium compounds. However, difficulties in purification of the resulting products led to low isolated yields (accounting only for the purest fraction collected). Yet, the cysteine-arylated products **oxa-5–7** were successfully characterized by NMR and mass spectrometry (SI).

Evaluation of the photophysical properties and DFT calculations

As depicted in Fig. 2 and Table 2, the photophysical properties of **oxa-1**–7 and **S1b** were studied in CH_2Cl_2. Oxazolinium **oxa-1** (R^1 = H) caused a red-shift of the absorption and emission, higher molar absorptivity (ε), and greater fluorescence quantum yield (Φ_F) compared to the non-cationic **S1b** (entries 1 and 2). Comparing **oxa-1** (R^1 = H) and **oxa-2** (R^1 = CH_3), the geminal methyl substituents of **oxa-2** demonstrated a negligible effect on the photophysical properties (entries 2 and 3). The electron donating –OMe group on R^2 of **oxa-3** gave red-shifted emission (480 nm), a larger Stoke shifts, and the highest Φ_F (0.51) (entry 4), while an electron withdrawing –Cl group on R^2 of **oxa-4** showed similar photophysical properties to **oxa-2** (entry 5 *vs.* entry 3). Thus, the substituents on R^2 showed significant effects on ε, emission, and Φ_F. In addition, **oxa-5–7** resulting from the substitution of *N*-Boc cysteine methyl ester with **oxa-2–4** exhibited red-shifted absorption and emission (entries 6–8). Notably, the

Table 2 Photophysical properties of **S1b** and **oxa-1–7** in CH_2Cl_2[a]

Entry	Compound	Max. abs (nm)	Max. Em (nm)	Stokes shift (nm)	ε (M^{-1} cm^{-1})	λ_{ex} (nm)	Φ_F[a]
1	**S1b**	295	310	15	12 100	270	0.06
2	**oxa-1**	363	413	50	22 400	360	0.35
3	**oxa-2**	363	413	50	36 900	360	0.33
4	**oxa-3**	365	480	115	68 000	365	0.51
5	**oxa-4**	363	413	50	35 200	360	0.34
6	**oxa-5**	380	425	45	42 000	370	0.09
7	**oxa-6**	380	500	132	30 700	365	0.40
8	**oxa-7**	380	430	50	46 500	365	0.07

[a] Quantum yields were measured using coumarin 153 (Φ_F = 0.54 in ethanol) as the standard reference.

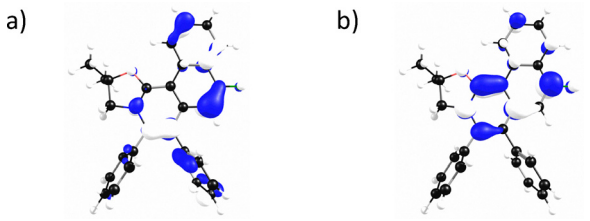

Fig. 3 (a) HOMO and (b) LUMO of **oxa-2**, isovalue = 0.05.

bright fluorescence images of **oxa-3** and **oxa-6** imply the potential application of **oxa-3** in fluorescent labelling and bioimaging (Fig. 2c). Moreover, the photophysical properties of **oxa-1–7** and **S1b** studied in 50 mM PBS (pH 7.4)/DMSO (9 : 1) also gave comparable results when using CH_2Cl_2 as a solvent (Fig. S2–S9 and Table S2, SI).

Based on the TD-DFT calculated electronic transitions, we simulated the absorption spectrum (Fig. S10a, red line, SI) for **oxa-2**. The simulated spectrum resembles the measured spectrum. TD-DFT calculations reveal that the lowest energy absorption band ($\lambda_{abs,cal}$ = 341 nm) originated from the HOMO → LUMO transition. The HOMO is mainly contributed by the π orbital of oxazolinium and the phenyl rings, whereas the LUMO is composed of the π* of the oxazolinium ring (Fig. 3). We have also simulated the emission spectrum (Fig. S10b, red line, SI) for **oxa-2**, where the calculated emission maximum (S_1 → S_0 transition, $\lambda_{em,cal}$ = 436 nm) is close to the measured value (λ_{em} = 413 nm).

Scope study for peptide modifications

A substrate scope study was conducted utilizing **oxa-3** due to its possession of the highest quantum yield among other analogues. Various cysteine-containing peptides were treated with **oxa-3** under the optimized conditions (Table 3). Up to 90%

Table 3 Scope study of different peptides with **oxa-3**[a]

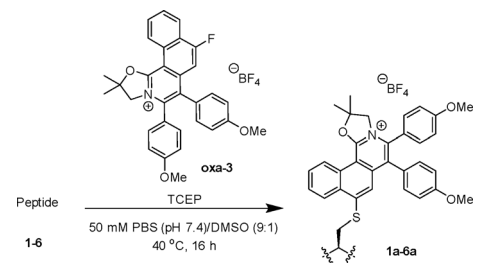

Entry	Peptide	Amino acid sequence	Product	Conv.[b] (%)
1	**1**	STSSSCNLSK	**1c**	90
2	**2**	AYEMWCFSQR	**2a**	69
3	**3**	KSTFC	**3a**	72
4	**4**	CSKFR	**4a**	89
5	**5**	CDPGYIGSR	5a	83
6	**6**	AYEMWCFHQR	**6a**	71
7	**7**	YTSSSKNVVR	7a	0

[a] Reaction conditions for modification: treatment of peptide (0.1 mM) with **oxa-3** (5 equiv.) in the presence of TCEP (1 equiv.) in 50 mM PBS buffer (pH 7.4)/DMSO (9 : 1) at 40 °C for 16 h. [b] Conversion was determined by LC-MS/MS analysis.

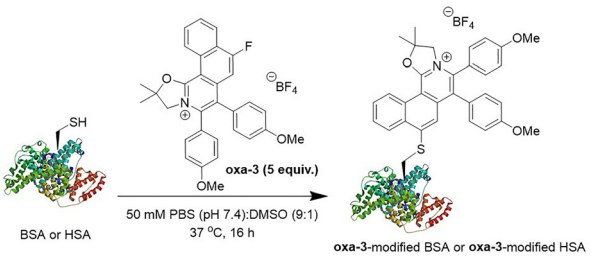

Scheme 3 S_NAr reaction of protein using **oxa-3**.

conversion was observed when various cysteine-containing peptides were treated (entries 1–7). No conversion was observed when peptide 7 (without cysteine) was employed (entry 7), indicating excellent cysteine selectivity.

Modification of proteins by fluorescent oxa-3

Next, **oxa-3** was utilized for protein modification of bovine serum albumin (BSA; PDB ID: 4F5S) and human serum albumin (HSA; PDB ID: 1AO6) with a single free cysteine residue at position 34 (Cys-34), without TCEP to maintain the structural integrity of proteins (Scheme 3). By LC-MS analysis, 60% conversion of **oxa-3**-modified BSA (Fig. S53 and S54, SI) and 70% conversion of **oxa-3**-modified HSA (Fig. S55 and S56, SI) were achieved after 16 h. Conversely, lysozyme (PDB ID: 3LYZ) remained intact after the reaction (Fig. S57 and S58, SI).

Analysis of protease-digested **oxa-3**-modified proteins showed that the reaction only occurred at Cys-34 of the targeted peptide fragments, while other amino acid residues remained intact (Fig. S59–S64, SI). SDS-PAGE analysis revealed a strong blue fluorescent signal for **oxa-3**-modified proteins while no signal was observed for native BSA and HSA at UV 365 nm (Table 4). Coomassie blue staining on the same gel gave deep blue colour signals of all native and modified proteins, indicating successful cysteine arylation of proteins by **oxa-3**. Both native and treated lysozyme had no fluorescence, stipulating excellent site-selectivity for peptide and protein modification.

Live cell imaging

Following the success of **oxa-3** in the provision of visual indication in protein modification, we sought to explore its applicability for cell imaging in biological systems. The cytotoxicity of **oxa-3** and **oxa-6** was evaluated at 24 h, showing moderate cytotoxicity to HeLa cells (IC_{50} = 16.11 and 14.54 μM, respectively, Fig. S66 and S67, SI). Then, the colocalization subcellular imaging of **oxa-3** and **oxa-6** was investigated at a non-cytotoxic concentration. HeLa cells were incubated with oxazoliniums (5 μM) in the presence of MitoTracker Red (MTR, 500 nM) for 15 min and washed with DPBS before the confocal imaging. As shown in Fig. 4, **oxa-3** and **oxa-6** showed remarkable cell permeability, intense green fluorescence, and good overlapping with MTR, with a Pearson's correlation coefficient value close to 0.8, indicating that **oxa-3** and **oxa-6** localized in the mitochondria.

Table 4 SDS-PAGE analysis of **oxa-3**-modified proteins

	UV 365 nm		Coomassie blue	
Protein	–	+	–	+
BSA				
HSA				
Lysozyme				

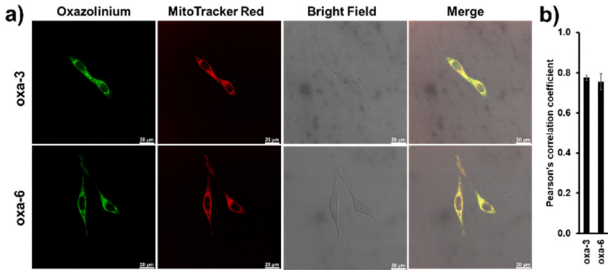

Fig. 4 (a) Live cell images of HeLa cells incubated with 5 μM **oxa-3** and **oxa-6** and 500 nM MTR for 15 min at 37 °C. The first and second columns indicate the green and red channels for oxazoliniums and MTR, respectively. The third column and the last column indicated bright-field images and merged images from the three channels, respectively. (b) Pearson's correlation coefficient of colocalization between oxazoliniums and MTR.

Due to the high concentrations of glutathione (GSH, 1–10 mM) present in the cells,[27] we studied the reactivity of **oxa-3** with GSH by incubating **oxa-3** (1 mM) with GSH (1 mM) for 15 min. Our results showed that 31% conversion was observed, indicating that the oxazoliniums have reactivity towards –SH containing biomolecules in cells (Fig. S69–S71, SI).

Conclusions

In conclusion, we have developed a series of fluorescent cationic fluorinated oxazoliniums for cysteine-selective arylation *via* an S_NAr reaction. Measurements of the photophysical properties and quantum yields presented **oxa-3**, with the electron-donating –OMe group, with a high quantum yield of 0.51. Under the optimized conditions, modifications of cysteine-containing peptides afforded up to 99% conversion. Finally, the applicability of **oxa-3** to provide visual indication for fluorescent labelling of cysteine-containing proteins and cell imaging was successfully demonstrated. This work highlights the potential of these fluorescent oxazoliniums for broad applications in chemical biology and biological studies.

Author contributions

K. K.-Y. K. and Y. T. L.: conceptualization, investigation, data curation, writing – original draft, and writing – review and editing; A. T.: investigation, formal analysis, and writing – original draft; J.-R. D.: formal analysis and writing – original

draft; L.-Y. T.: investigation; M.-K. W.: conceptualization, funding acquisition, supervision, and writing – review and editing.

Conflicts of interest

There are no conflicts to declare.

Data availability

The data supporting this article have been included as part of the supplementary information (SI). Supplementary information: details of experimental procedures, LC-MS analyses, DFT data and NMR data. See DOI: https://doi.org/10.1039/d5cb00289c.

Supplementary data have been deposited with the Protein Data Bank.[28–30]

Acknowledgements

We gratefully acknowledge the financial support from the Research Grants Council of the Hong Kong Special Administrative Region, China (PolyU15300520), the PolyU Postdoc Matching Fund Scheme (P0043412: W262), the InnoHK initiative of the Innovation and Technology Commission of the Hong Kong Special Administrative Region Government, the State Key Laboratory of Chemical Biology and Drug Discovery, The Hong Kong Polytechnic University (P0053072: ZZV2), the University Research Facility in Life Sciences (ULS) and the University Research Facility in Chemical and Environmental Analysis (UCEA) of PolyU. We would like to thank Prof. F. K.-C. Leung from Department of Applied Biology and Chemical Technology (ABCT) of The Hong Kong Polytechnic University for hardware support during the *in vitro* and cell imaging experiments.

References

1 C. D. Spicer and B. G. Davis, *Nat. Commun.*, 2014, **5**, 4740.
2 N. Stephanopoulos and M. B. Francis, *Nat. Chem. Biol.*, 2011, **7**, 876–884.
3 L. R. Malins, *Curr. Opin. Chem. Biol.*, 2018, **46**, 25–32.
4 S. B. Gunnoo and A. Madder, *ChemBioChem*, 2016, **17**, 529–553.
5 C. Zhang, E. V. Vinogradova, A. M. Spokoyny, S. L. Buchwald and B. L. Pentelute, *Angew. Chem., Int. Ed.*, 2019, **58**, 4810–4839.
6 W. Lin, X. Ding, J.-W. Han, L.-S. Yu and F.-J. Chen, *Org. Chem. Front.*, 2025, **12**, 2777–2789.
7 A. M. Spokoyny, Y. Zou, J. J. Ling, H. Yu, Y.-S. Lin and B. L. Pentelute, *J. Am. Chem. Soc.*, 2013, **135**, 5946–5949.
8 Y. Zou, A. M. Spokoyny, C. Zhang, M. D. Simon, H. Yu, Y.-S. Lin and B. L. Pentelute, *Org. Biomol. Chem.*, 2014, **12**, 566–573.
9 S. Kalhor-Monfared, M. Jafari, J. Patterson, P. Kitov, J. Dwyer, J. Nuss and R. Derda, *Chem. Sci.*, 2016, **7**, 3785–3790.
10 D. Gimenez, C. A. Mooney, A. Dose, G. Sandford, C. R. Coxon and S. L. Cobb, *Org. Biomol. Chem.*, 2017, **15**, 4086–4095.
11 W. Liu, Y. Zheng, X. Kong, C. Heinis, Y. Zhao and C. Wu, *Angew. Chem., Int. Ed.*, 2017, **56**, 4458–4463.
12 T. Tsunemi, S. J. Bernardino, A. Mendoza, C. G. Jones and P. G. Harran, *Angew. Chem., Int. Ed.*, 2020, **59**, 674–678.
13 B. M. Lipka, V. M. Betti, D. S. Honeycutt, D. L. Zelmanovich, M. Adamczyk, R. Wu, H. S. Blume, C. A. Mendina, J. M. Goldberg and F. Wang, *Bioconjugate Chem.*, 2022, **33**, 2189–2196.
14 S. Casa and M. Henary, *Molecules*, 2021, **26**, 1160.
15 S. Zeng, X. Liu, Y. S. Kafuti, H. Kim, J. Wang, X. Peng, H. Li and J. Yoon, *Chem. Soc. Rev.*, 2023, **52**, 5607–5651.
16 F. de Moliner, F. Nadal-Bufi and M. Vendrell, *Curr. Opin. Chem. Biol.*, 2024, **80**, 102458.
17 G.-Q. Jin, J.-X. Wang, J. Lu, H. Zhang, Y. Yao, Y. Ning, H. Lu, S. Gao and J.-L. Zhang, *Chem. Sci.*, 2023, **14**, 2070–2081.
18 P. Gandeepan and C. H. Cheng, *Chem. – Asian J.*, 2016, **11**, 448–460.
19 P. Karak, S. S. Rana and J. Choudhury, *Chem. Commun.*, 2022, **58**, 133–154.
20 R. Sanjana, J. Jayakumar and K. Parthasarathy, *Asian J. Org. Chem.*, 2025, e202500177.
21 C. Z. Luo, P. Gandeepan, J. Jayakumar, K. Parthasarathy, Y. W. Chang and C. H. Cheng, *Chem. – Eur. J.*, 2013, **19**, 14181–14186.
22 J.-R. Deng, W.-C. Chan, N. C.-H. Lai, B. Yang, C.-S. Tsang, B. C.-B. Ko, S. L.-F. Chan and M.-K. Wong, *Chem. Sci.*, 2017, **8**, 7537–7544.
23 W.-M. Yip, Q. Yu, A. Tantipanjaporn, W.-C. Chan, J.-R. Deng, B. C.-B. Ko and M.-K. Wong, *Org. Biomol. Chem.*, 2021, **19**, 8507–8515.
24 A. Tantipanjaporn, K.-Y. K. Kung, J.-R. Deng and M.-K. Wong, *Spectrochim. Acta, Part A*, 2024, **319**, 124524.
25 L.-Y. Tsang, A. Tantipanjaporn, K. K.-Y. Kung, H.-Y. Sit, W. Y. O, A. K.-H. Chan, N. C.-H. Lai and M.-K. Wong, *Adv. Synth. Catal.*, 2025, **367**, e70023.
26 M. N. Holerca and V. Percec, *Eur. J. Org. Chem.*, 2000, 2257–2263.
27 C.-Y. Cui, B. Li and X.-C. Su, *ACS Cent. Sci.*, 2023, **9**, 1623–1632.
28 A. Bujacz, Structures of bovine, equine and leporine serum albumin, *Acta Crystallogr., Sect. D: Biol. Crystallogr.*, 2012, **68**, 1278–1289, DOI: 10.1107/S0907444912027047.
29 S. Sugio, A. Kashima, S. Mochizuki, M. Noda and K. Kobayashi, Crystal structure of human serum albumin at 2.5 A resolution, *Protein Eng.*, 1999, **12**, 439–446, DOI: 10.1093/protein/12.6.439.
30 R. Diamond, Real-space refinement of the structure of hen egg-white lysozyme, *J. Mol. Biol.*, 1974, **82**, 371–391, DOI: 10.1016/0022-2836(74)90598-1.